1 Scintillation and Inorganic Scintillators

Abstract. This chapter introduces the basic definitions and gives the minimum necessary information about the phenomenon of scintillation and the mechanisms which have to be taken into account for the development of scintillation materials. It starts with an historical brief and describes the sequence of the processes leading to scintillation in a dielectric medium. Definitions are then given of the parameters related to the physical process of light production in the medium and not dependent on the shape, surface state and optical quality of the scintillator block. After a survey of scintillation mechanisms it is shown that several self activated scintillators show better scintillation properties when they are doped by appropriate ions. A description is given of the most important activators with a discussion about the conditions for the activator to be efficient in a host matrix. As an example the electron energy level structure of Ce^{3+} and Pr^{3+} ions is described. It is shown that these two ions are good activators with a bright and fast scintillation in many compounds. Several approaches to classify scintillation materials are discussed. This chapter is concluded with a list of the scintillation materials developed so far and of their most important properties.

1.1 The Phenomenon of Scintillation

What is a scintillator?

For a long time the answer to this apparently simple question did not find a clear and unambiguous formulation.

Scintillators have played a major role in the development of modern physics. The visual observation of scintillation on a zinc sulfide screen has allowed E. Rutherford to observe α particles, an event which can be considered as the starting point of modern nuclear physics. Till the end of the Second World War, zinc sulfide and calcium tungstate were among the most popular particle detectors found in nuclear physics laboratories. The intensive development of atomic projects in the postwar period stimulated the development of new ionizing-radiation – detecting technique, including scintillation counters. With the development of experimental physics, and in particular with the occurrence of the photoelectric multipliers, it became clear that scintillating materials are ideal devices to detect elementary particles and to measure their parameters [1–3]. In a rather short time (1947–51) it has been discovered that scintillation can be observed in various organic and

inorganic crystalline media [4–7], as well as in fluids [8–11], gases [12, 13], and polymeric compounds [14]. At the same time the still most widely used scintillating crystalline material NaI (Tl) [15] has been discovered.

Kallmann [5] has made an attempt to specify the essential parameters of scintillation materials. He made, in particular, the distinction between

(a) the physical light output, which corresponds to the fraction of the absorbed ionizing radiation energy which is transformed into light, and
(b) the technical light output, which is the amount of light actually collected at the extremity of a scintillation element, taking into account all factors of light collection and absorption in the medium.

He defined scintillation as flashes of light in phosphorus. In the Physical Encyclopedia [16], scintillation is defined as "the short light flashes originating in a scintillator under the effect of ionizing radiation." Fünfer and Neuert [17] defined scintillation as "the phenomenon of luminescence in transparent solids, fluids or gases, originating at the propagation of the ionizing radiation through them."

One shall remark that all these definitions of scintillation have some shortcomings. First of all, they are restricted to the phenomenology of light production under excitation by ionizing radiation but they do not consider the mechanism of energy transfer and conversion into light. From this point of view, Cherenkov radiators [18] could be considered as scintillators, which is fundamentally incorrect. A second limitation results from the confusion between scintillation and luminescence, which is at the origin of a semantic imprecision between scintillators and luminophores. Although for the end user "there is no difference between a scintillator and a fluorescent lamp," according to A. Lempicki, there is nevertheless an important difference in the mode of excitation and energy relaxation.

The mechanism of luminescence, which is exploited in fluorescent lamps and in lasers, results from the radiative relaxation of an active ion of the material after the direct excitation between its fundamental state and excited energy levels by an electrostatic discharge or a pulse of light. On the other hand the origin of the scintillation is the energy loss of ionizing radiation through matter.

Electrons and γ quanta lose energy when traversing a medium by the three fundamental mechanisms of electromagnetic interactions:

(a) photoabsorption,
(b) Compton scattering, and
(c) electron–positron pair formation.

The interaction cross section through each of these mechanisms is energy dependent [19], photoabsorption and Compton scattering being dominant at low and medium energy and pair formation at high energy with an onset at 1.02 MeV, the mass energy of an electron–positron pair at rest. Neutral particles and charged hadrons lose energy mainly through direct interactions with

nuclei or ionization of atoms for charged particles. Knock-on electrons or γ or β decay from the relaxation of nuclei excited by neutron or neutrino capture will then lose energy through the standard electromagnetic interactions described above. As long as the energy of particles is high enough for multiple scattering and electron–positron pair creation, their energy is progressively distributed to a number of secondary particles of lower energy which form an electromagnetic shower. Below the threshold of electron–positron pair creation, electrons will continue to lose energy through Compton scattering. In the case of an ordered material like a crystal, another mechanism takes place at this stage. The electrons in the keV range from the shower will start to couple with the electrons and atoms of the lattice. They will excite the electrons from the occupied electronic states of the material (valence or deeper bound states) at different levels in the conduction band. At each of these interactions, an electron–hole pair is created. If the energy of the electron is high enough to reach the ionization threshold, we have then free carriers which will move randomly in the crystal until they are trapped by a defect or recombine on a luminescent center. In the case the ionization threshold is not reached the electron and hole will cool their energy by coupling to the lattice vibration modes until they reach the top of the valence band for the hole and the bottom of the conduction band for the electron. They can also be bound and form an exciton whose energy is in general slightly smaller than the bandgap energy. At this stage the probability is maximum for a coupling to luminescent centers through either an energy or a charge transfer mechanism.

For a material to be a scintillator it must contain luminescent centers. They are either extrinsic, generally doping ions, or intrinsic, i.e. molecular systems of the lattice or of defects of the lattice which possess a radiative transition between an excited and a lower energy state. Moreover, the energy levels involved in the radiative transition must be contained in the forbidden energy band, to avoid reabsorption of the emitted light or photo-ionization of the center.

In a way, a *scintillator* can be therefore defined as a wavelength shifter. It converts the energy (or wavelength) of an incident particle or energetic photon (UV, X-ray, or gamma-ray) into a number of photons of much lower energy (or longer wavelength) in the visible or near visible range, which can be easily detected with current photomultipliers, photodiodes, or avalanche photodiodes.

In contrast to Cherenkov radiation, scintillation occurs as the result of a chain of processes which are characterized by different time constants. This is well described by Vasiliev [20] and will be discussed in details in Chap. 4, taking into account the existence of thresholds of "hot" electrons and holes inelastic interactions. Four essential phases are distinguished and listed in Table 1.1.

Table 1.1. The sequence of processes leading to scintillation in a medium

Phase	Characteristic Time, s
1 *Energy conversion:* Initial energy release with formation of "hot" electrons and holes	$\tau_1 = 10^{-18} - 10^{-9}$
2 *Thermalization:* Inelastic processes of interaction of "hot" electrons and holes and their thermalization	$\tau_2 = 10^{-16} - 10^{-12}$
3 *Transfer to luminescent centers:* Formation of excitonic states and groups of excited luminescent centers	$\tau_3 = 10^{-12} - 10^{-8}$
4 *Light emission:* Relaxation of excited luminescent centers and emission of scintillation light	$\tau_4 > 10^{-10}$

The initial energy release in a medium occurs in a wide time range; however, its duration cannot be smaller than $2R/c$, where $R \sim 10^{-10}$ m is the order of atomic radius and c is the light speed. It also cannot exceed the transit time of the particle or γ-quantum in the scintillator and, for crystalline inorganic compounds, is restricted to a few nanoseconds. It must be noticed at this stage that the transfer to the detecting medium of at least a fraction of the energy of a particle does not necessarily require the transit of that particle through the medium. The transverse electrical field associated with a relativistic particle traveling close to the surface of a dielectric inorganic scintillator can in fact penetrate the medium and therefore interact with the electrostatic field of the crystal. This phenomenon could be exploited for the monitoring of intense particles beams near a flat surface or through nanotubes [21].

The "hot" electrons and holes inelastic scattering processes and their thermalization are rather fast in heavy crystals generally used as scintillating materials which are characterized by a high density of electronic states.

The formation of excitonic states and the transfer of their excitation to luminescent centers occur with characteristic time constants which are generally in the picosecond range.

At the end of the process the relaxation of the excited luminescent centers and the corresponding light emission is characterized by time constants distributed in a wide time range which are determined by the quantum wavefunction characteristics of the different levels involved in the transitions.

It must be noticed here that the excitation of the scintillation by a charged particle does not necessarily require direct impact of the particle with the electrons and nuclei of the scintillation medium. Energy is transferred from the particle to the scintillation through the electromagnetic field associated to the particle. It is therefore possible to excite the luminescence of a scintillator by a relativistic particle (the transverse extention of the electromagnetic wave is larger in this case) travelling very close to its surface without penetrating it.

Therefore, *scintillation* is a luminescence induced by ionizing radiation in transparent, dielectric media.

This complex sequence of phenomena characterizes the scintillation process, contrary to the photoluminescence which results from the direct excitation of the luminescent centers.

The kinetics is therefore more complex in many cases, contrary to what can be observed in gases, condensed gases, fluids, and their vapors. In such media the atoms of the gas or molecules of organic dyes or anionic complexes of rare-earth ions can be considered to some extent as free with almost no interaction with other particles of the medium. The luminescence decay time is therefore equal to the radiating decay time τ_r of luminescent centers excited states. It means that all the light quanta have been emitted after a few τ_r. On the other hand, crystalline compounds are characterized by a noncontinuous electronic energy distribution with an energy gap $E_g \gg kT$, separating a filled valence electronic band from higher energy and generally not populated levels forming the conduction band. The width of the forbidden band between the valence and the conduction band determines if the material is a semiconductor ($<$ 2–3 eV) or an insulator ($>$3 eV, typically $\geq$4 eV).

For a given material, a plurality of luminescent centers, whose radiating levels are localized in the forbidden zone, can coexist and interfere with each other. Some of these luminescent centers are cations or anionic complexes of the lattice or doping ions such as Ce^{3+} specifically introduced at the crystal growth. Some others are generated by the interaction of the ionizing radiation with the medium. Such induced centers play an important role in the scintillation as they can sensitize or quench luminescence or act as electron or hole donors for existing radiating centers via a secondary excitation process. In practice this secondary excitation is generated not only by direct Coulomb interaction but also by thermoactivation or electron tunneling from matrix host defects which trap electrical carriers produced by the incident particle. The kinetics of primary and secondary excitation processes are different. If we define ω_{int} as the frequency of interaction between primary and secondary luminescent centers in the medium, we can distinguish different cases, depending on how the mean time between interactions compares with the time of formation of primary excited luminescent centers τ_3 and with their radiating decay time τ_r.

For

$$1/\omega_{int} \sim \tau_3 \ll \tau_r \ , \tag{1.1}$$

the kinetics of the direct scintillation will dominate, characterized by a very fast rise time followed by a single exponential decay, the signature of the radiative relaxation of the luminescent center.

If on the other hand

$$1/\omega_{int} \gg \tau_r \quad \text{and} \quad 1/\omega_{int} \gg \tau_3 \ , \tag{1.2}$$

which is frequently the case in real materials, the direct scintillation is accompanied by a phosphorescence which results from the delayed decay of the secondary luminescent centers. The interaction of luminescent centers between themselves or with charge carriers traps leads to a more complex kinetics with generally longer rise time and strong nonexponential decay with long tails in some cases. As a measure of the contribution of phosphorescence in scintillation, the afterglow parameter is used. *Afterglow* is the amplitude of the luminescence signal, excited by ionizing radiation and measured after a fixed time, for example $10 \cdot \tau_{\mathrm{r}}$.

Scintillation is characterized by several parameters. Some of them depend on the shape, surface state, and optical quality of the scintillator block. We list here those which are related to the physical process of light production in the medium.

1.1.1 Scintillation Yield

Following [22,23] we define the quantum yield or the light yield of scintillation Y as the amount of light quanta emitted by a scintillator per unit energy deposited by ionizing radiation in the medium. Thus,

$$Y = \prod_i y_i \ , \tag{1.3}$$

where y_i are the yields of the processes given in Table 1.1.

The yields of the first two processes have been analyzed by the authors [24–29]. The models show approximately the same limiting yields [23] but their experimental measurement is not easy as it is difficult in practice to decouple these processes from luminescence quenching in real crystalline materials. A phenomenological approach leads to the following formulation:

$$y_1 \cdot y_2 = \frac{E_\gamma}{\beta \cdot E_{\mathrm{g}}} \ ,$$

where $\beta \cdot E_{\mathrm{g}}$ is the mean energy necessary for the formation of one thermalized electron–hole pair in a medium with a forbidden zone of width E_{g} and E_γ is the absorbed energy.

The yield of the formation of radiating centers S is defined by the efficiency of the energy transfer of thermalized pairs to the excited states of luminescent centers.

Finally we define Q as the quantum yield of the intracenter luminescence. Hence,

$$Y = \frac{E_\gamma}{\beta \cdot E_{\mathrm{g}}} S \cdot Q \tag{1.4}$$

and the energy efficiency of scintillation Y_{e} is

$$Y_{\mathrm{e}} = \frac{E_f}{\beta \cdot E_{\mathrm{g}}} S \cdot Q \ , \tag{1.5}$$

where E_f is the average energy of scintillation photons. There is therefore a clear advantage of having a host with a small bandgap. In this case however, the risk of photo-ionization of the activator increases if its ground or excited states are too close to the valence or conduction bands respectively. The density of traps in the forbidden band also increases which generally reduces the scintillator yield. P. Dorenbos [146] has calculated a maximum theoretical scintillator yield of 140,000 photons/sec in an ideal Ce^{3+} doped scintillator with a small bandgap, just large enough to host the Ce^{3+} optimal transition.

These expressions become more complex if we take into account additional mechanisms of energy losses, for instance surface losses in a medium [30, 31], and the structure of the density of states in the valence and in the conduction bands [20].

1.1.2 Kinetics of Scintillations

The kinetics of scintillation $I(t)$ is defined as the law of the variation in time of the scintillation light intensity and its magnitude $I = \int I(t)\,dt$ is proportional to Y. It is related to the time variation of the population of the excited states of the luminescent centers. For a simple process, with only one radiating center and no interaction between luminescent centers and traps, the decay is exponential and characterized by a time constant τ_{sc}, the time after which the amplitude has decreased by a factor e. For two independent radiating centers the same description with two exponentials is also valid. But in real cases the situation is very often more complex, involving energy transfer between centers and quenching mechanisms, and the resulting light emission is strongly nonexponential. It is nevertheless a common practice to describe this complex emission curve by a series of exponentials with different time constants. This has in most of the cases no physical justification but simplifies the calculations.

1.1.3 Radioluminescence Spectrum

This is the wavelength (or frequency or energy) distribution of the scintillation light when the medium is excited by ionizing radiation. It is generally composed of a series of emission bands which are each characterized by their maximum λ_{sc} or ν_{sc} and half-width $\Delta\lambda_{sc}(\Delta\nu_{sc})$ at a given temperature. Radioluminescence is also called cathodoluminescence in reference to the first observations of scintillation at the cathode of an electron gun.

1.1.4 Photoluminescence Spectrum

This is the wavelength (or frequency or energy) distribution of the scintillation light when the medium is excited by photons of energy below the ionization energy of the atoms. This information combined with the structure of the excitation spectrum, generally up to a few tens of eV, is very

useful to determine the energy levels involved in the excitation and relaxation mechanisms. On the other hand, one has to be very careful not to draw too rapid conclusions about the properties of the scintillator on the basis of the photoluminescence spectrum only which does not reflect at all the mechanisms of energy transfer and thermalization in the medium. This error is frequently made and leads to several misinterpretations. In the most dramatic case we can find materials with a good photoluminescent yield when excited in the UV range but with no light emitted under gamma-rays excitation. A typical example is given by the tungstate group which exhibits good scintillation properties in some host matrices ($CaWO_4$, $CdWO_4$, $PbWO_4$) and no scintillation at all in some other compounds ($BaWO_4$).

1.2 Survey of Scintillation Mechanisms

As already explained, the mechanisms of excitation of the luminescent centers in a scintillator as well as their properties are strongly influenced by the surrounding medium, particularly if this is a solid, and even more in the case of a crystal with a regular structure. Fundamental aspects of this phenomenon will be discussed in details in Chap. 4. Here we give a survey of scintillation mechanisms. The coupling between the lattice and the luminescent center is essential in the way the energy is transferred between them in both directions. In particular the conditions of localization and delocalization of excitations are strongly affected by the positions of the luminescent centers energy levels relative to the valence and conduction bands formed by the orbitals of the lattice atoms. This is well illustrated for instance by the modifications of the luminescent properties of activating ions such as Ce^{3+} depending on the type of ligand and on the strength and the symmetry of the crystalline field in different host materials.

Electrons and holes produced by ionizing radiation have several ways to be involved in the scintillation process after their thermalization:

1. $e + h \rightarrow h\,\nu$,
2. $e + h \rightarrow ex \rightarrow h\,\nu$,
3. $e + h + A \rightarrow ex + A \rightarrow A^{*} \rightarrow A + h\,\nu$,
4. $e + h + A \rightarrow A^{1+} + e \rightarrow A^{*} \rightarrow A + h\,\nu$,
5. $e + h + A \rightarrow (A^{1-})^{*} + h \rightarrow A + h\,\nu$,
6. $A \rightarrow A^{*} \rightarrow A + h\,\nu$

The simplest emission process (1) is the result of the direct radiative recombination of free thermalized electrons in the conduction band with holes from the valence band or from deeper electronic shells. Usually the ionizing radiation produces deep holes in the lattice which are progressively converted into holes of smaller energy through a succession of Auger conversions. Similarly hot electrons from the first interaction are cooled down to the bottom of the

conduction band by inelastic interactions. In most of the cases the recombination takes place when the energy of the electron and hole has sufficiently decreased so that they bind to each other, creating an exciton with an energy slightly smaller than the bandgap.

However, for certain configurations of the valence and core atomic electron bands the Auger conversion cannot take place and the electron recombines directly with a deep hole, giving rise to a fast UV emission [32–34]. Such kind of radiating recombination is called cross-luminescence and it is observed in some wide band gap fluoride and chloride crystals.

Thermalized carriers can also be bound in some places of the lattice, for instance, in the vicinity of a specific atom or a structural defect (2). They are called autolocalized excitons (*ex*) and their radius, small or large, depends on the electrostatic field in this configuration. In many inorganic compounds these excitons have a radiative decay channel [35]. The luminescence of free excitons or bound excitons is generally absent in complex compounds and has been observed so far only in simple oxides [36, 139].

Under certain conditions in the presence of impurity centers or activating ions A the exciton luminescence is efficiently quenched, causing thus a sensitization of the luminescence of the activating ions A(3). In this case the excitation of radiative centers results from an energy transfer from excited matrix states.

The process competing to the formation of excitons is the direct capture of free thermalized carriers, electrons (4) or holes (5) by activating ions A with the subsequent formation of their excited state A^*. The cross section for electron or hole capture depends on the nature of the activating ion and on the structure of the local electrostatic field in its vicinity. In contrast to the previous case the excitation of radiating centers is now the result of a charge transfer mechanism from excited matrix states.

Finally the direct excitation of activating centers by ionizing radiation (6) provides an important contribution to the scintillation in the case of heavy doped or self-activated scintillators. A typical example is cerium fluoride (CeF_3).

Besides these mechanisms, an intrazone luminescence caused by radiating transitions of hot electrons and holes from the conduction and valence bands has also been reported [37]. This luminescence is distributed in a wide spectral region and characterized by a low yield, independent of the temperature, of typically 10^{-3}–5×10^{-6} eV/eV in $NaNO_3$ and $BaMgAl_{10}O_{17}$ crystals. The decay time τ_{sc} is very fast, of the order of a few nanoseconds only.

The efficiency of activated scintillators is strongly dependent on the ratio of the bandgap in the crystal to the energy of the activator radiating state as well as on the relative position of its ground and excited states to the top of valence band and to the bottom of the conduction band, respectively. The first requirement for an activator with an excited state energy E_r to be efficient in a host matrix with a bandgap E_g is

$$E_{\mathrm{g}} \geq E_{\mathrm{r}} \,. \tag{1.6}$$

This condition prevents the reabsorption of the luminescence in the medium, at least if the crystal is free from impurities or structural defects having energy levels in the bandgap.

Another condition to avoid the delocalization of electrons in the conduction band from the activator excited state is related to the energy gap ΔE between the radiating level of the doping ion and the bottom of the conduction band.

Thus,

$$\Delta E \leq 0, \quad \text{the scintillation yield } Y = 0 \,, \tag{1.7}$$

$$\Delta E > 0, \quad \text{the scintillation yield } Y \geq 0 \,. \tag{1.8}$$

Moreover, if

$$\Delta E \gg kT \quad \text{or} \quad \tau_{\mathrm{r}} \ll \tau_{\mathrm{d}} \,, \tag{1.9}$$

where the delocalization time $\tau_{\mathrm{d}} \approx (1/S)\exp(-\Delta E/kT)$, with S is the frequency factor, k is the Boltzman constant, and T is the temperature, the scintillation yield is not strongly dependent on the temperature. In the reverse case, one can anticipate a reduction of the scintillation yield when the temperature increases (temperature quenching).

The energy gap between the ground state of the activating ion and the top of the valence band plays also an essential role in the hole capture by the activator through the mechanism (4). In the case of a ground state localization in the valence band, the hole remains delocalized and its trapping never occurs. If on the other hand the activator ground state lies too high above the valence band, the probability of hole capture by the radiating center is low, resulting in a poor efficiency of the scintillator.

The characteristic decay time for the direct electron–hole recombination (1) does not exceed a few nanoseconds if the final state involves a core atomic band. If on the other hand there is a participation of the valence band in the direct or excitonic recombination (1,2), the scintillation, as a rule, is characterized by slowly decaying kinetics due to radiating recombination process with characteristic time constants in the μs–ms region. The fact that some self-activated scintillators, like $PbWO_4$ [38], exhibit a fast room temperature scintillation in the nanosecond range is only the consequence of a luminescence-quenching mechanism competing with the radiative relaxation of the excitation. In this case the decay is nonexponential, which is a common signature of temperature-quenched scintillators.

In the case of radiating transitions in the simple model of the dipole electrical transition the lifetime of the activator luminescence (radiant time) is defined by the well-known formula:

$$\tau_{\mathrm{r}} \sim 1/(\nu^3 \langle \Psi_A \,|d|\, \Psi_A^* \rangle^2) \tag{1.10}$$

where $\langle \Psi_A | d | \Psi_A^* \rangle$ is the operator of the dipole electrical transition between the excited and ground states of the activating ion and ν is the frequency of the transition. The general expression is given in [39]:

$$\tau_{\mathrm{r}} = \frac{1.5 \times 10^5 \lambda^2}{f \frac{1}{9}(n^2+2)^2 \, n} \, , \tag{1.11}$$

where f is oscillator strength, λ is averaged wavelength of transition equal to $1/\nu$, and n is index of refraction of the medium.

When the requirements (1.8) and (1.9) are satisfied and in the absence of quenching mechanisms the radiating time is close to the radiant time. Figure 1.1 shows the room temperature radiant (τ_{r}) and scintillation (τ_{sc}) time of the interconfiguration $5d \rightarrow 4f$ transition of the Ce^{3+} ion in different crystals as a function of the frequency ν of the peak of the luminescence. GSO and YSO have two different coordinations of Ce^{3+} with different maxima and kinetics of the luminescence. The luminescence decay time correlates well with a square-law dependence of the radiating time with the frequency of the peak of the luminescence band.

On the other hand, the values for the scintillation decay time τ_{sc} are in some cases very different from the intracenter-excited luminescence radiating

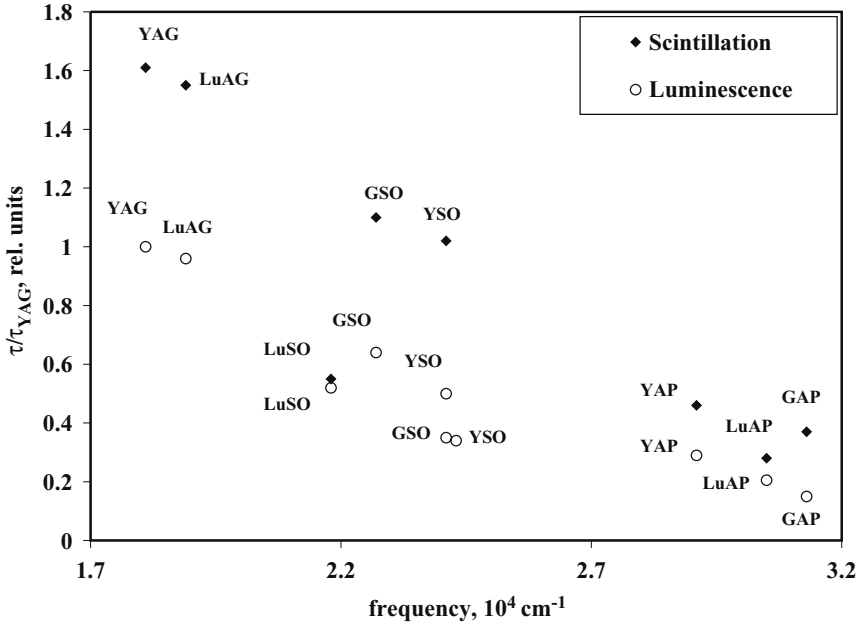

Fig. 1.1. Luminescent decay time τ_{r} of the interconfiguration $5d \rightarrow 4f$ transition of the Ce^{3+} ion and scintillation decay time τ_{sc} versus frequency ν of the luminescence band maximum at room temperature. Data are taken from [42–48]

time. This is caused by the time needed to transfer the energy to the radiating centers through the different mechanisms described in this paragraph. If this transfer occurs preferentially through the energy transfer mechanism, the decay time of scintillation is closer to the radiating time of the activator. This is explained within the Förster–Dexter model [40, 41] describing the sensitization of activating ions by randomly distributed donors in the crystal. According to the model the luminescence kinetics in a dipole approximation is described by the expression

$$I(t) = I_0 \exp[-(t/\tau_\mathrm{r}) + 4\sqrt{t}\pi^{3/2} N_\mathrm{a} (C_\mathrm{DA})^{1/2}/3 + \bar{w}t] \,, \tag{1.12}$$

where N_a is the concentration of activators, C_DA is a parameter of donor–acceptor dipole–dipole interaction, and $\bar{\omega}$ the rate of migration-restricted energy transfer. For a large migration rate $\bar{\omega}$ and interaction probability C_DA, the rise time of the scintillation is fast and the scintillation kinetics approaches the intracenter-excited luminescence kinetics.

For the direct recombination of thermalized electrical carriers as well as for the excitonic emission according to the processes (1) and (2), the peak emission of the scintillation correlates with the band-gap value. The set of possible radiating states is in this case limited to excited levels of metallic ions of the host matrix, polaronic or excitonic states, or shallow traps. All these states are located near the bottom of the conduction band. As the relaxation involves energy levels situated at the top of the valence band, the energy of the transition is generally close to the bandgap energy. However, the interaction of the electrostatic field of the lattice with the radiating center, which is in practice different for the excited and the ground state, introduces a modification of the orbital configurations through vibronic interactions [49]. This effect results in a shift of the luminescence band maximum to longer wavelength (the Stockes shift). Figure 1.2 shows the wavelength of the scintillation band maximum of various undoped scintillation crystals versus their respective bandgap energy.

In doped crystals the luminescence properties of the doping ions can be predicted by the effect of the crystalline field for ions of the iron group [50,51] and for the rare-earth ions in the frame of the model described in [52]. It has been shown that for a given crystalline matrix the energy difference between the first excited state $4f^{n-1}5d$ and the ground state configuration $4f^n$ is given by

$$\Delta_{fd} = \Delta^0_{fd} - \sigma_2 S_\mathrm{host} \tag{1.13}$$

where Δ^0_{fd} is the energy difference between the first excited state $4f^{n-1}5d$ and the ground state configuration $4f^n$ of a free ion, and S_host is the parameter defined by the specificity of the matrix host,

$$\sigma_2 = [\langle 4f^{n-1}5d \left| r^2 \right| 4f^{n-1}5d\rangle - \langle 4f^n \left| r^2 \right| 4f^n\rangle] \sum_i \alpha_i Z_i e^2/R_i^6 \,, \tag{1.14}$$

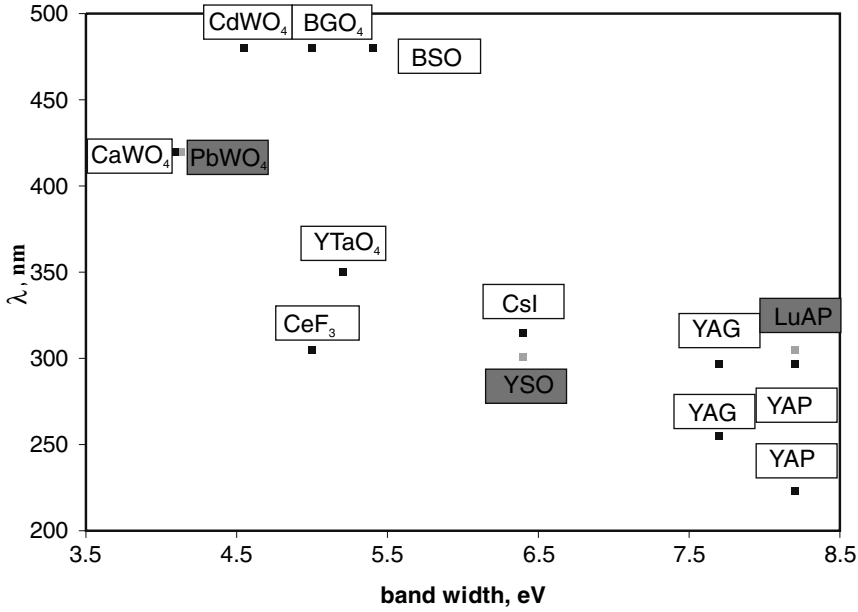

Fig. 1.2. Luminescence band maxima of various undoped scintillation crystals versus band gap. The data from [55–57] have been used

where Z_i is the quantity of ligands with polarizability α_i and distance R_i from the doping ion. Using this expression, the authors of reference [53] have shown that the energy of the first excited state $4f^{n-1}5d$ of any trivalent rare-earth ion of the Lanthanide family scales with the one of the Ce^{3+} ion and is equal to

$$\Delta_{fd}(Ln^{3+}) = C\Delta_{fd}(Ce^{3+}) + B\,, \tag{1.15}$$

where B and C are independent of the crystal parameters constants. The decrease of this energy for a given crystalline compound is about the same for all rare-earth ions because σ_2 is about the same for all lanthanides and S_{host} depends only on lattice parameters of the compound.

The surveyed model has found convincing confirmation in the analysis of spectroscopic parameters of trivalent rare-earth ions in more than 300 various compounds [54,58,59]. The basic conclusion concerning interconfiguration optical transitions in trivalent rare-earth ions is that the effects of the crystalline matrix and of the activator ion on the parameters of the optical transition are independent. Thus, knowing the energy of one allowed interconfiguration transition of any of the rare-earth ions, for example Ce^{3+} in a given matrix, it is possible to calculate similar transitions for another Lanthanide ions in the same crystalline compound.

1.3 Scintillation-Radiating Centers

We will consider here the different impurity ions which can activate a scintillator. Several self-activated scintillators show better scintillation properties when they are doped by appropriate ions. As explained in the previous paragraph, there are some conditions to be met for the activator to be efficient in a host matrix. These conditions are related to the position of the activator energy levels involved in the luminescence relative to the conduction and valence bands of the matrix. More generally the two basic practical requirements are the stability of the charge states of the luminescent center in the host and the high-quantum yield of the intracenter luminescence. They limit the number of centers to be considered and exclude, for instance, point structure defects associated to the substitution of a host matrix ion by an activator ion with a different valence state (nonisovalent doping), however, do not guarantee an efficient scintillation yield through the activation of the specific centers of a crystal.

1.3.1 Ions of the Iron Group

Radiating transitions in these ions arise between the Stark components of the $3d^n$ electronic configurations. As the $3d^n$ shell is the outer shell for the light ions of this group, the effect of the crystalline field is stronger than the spin–orbit interaction. The peak position of the luminescence band is therefore rather sensitive to the strength of the crystalline field created by the coordination of the ligands. The energies of the Stark components of the terms of the $3d^n$ configurations depend on the strength of the crystalline field. They are described by the Tanabe–Sugano diagrams [50] and discussed explicitly in the literature [60].

The lightest ion of the iron group is the titanium. Its trivalent ion Ti^{3+}has the $3d^1$ electronic configuration and is localized in an octahedral oxygen coordination. Its wide luminescence band with a maximum of 790 nm is observed in the garnet $Y_3Al_5O_{12}$. In the yttrium perovskite crystal $YAlO_3$ the Ti^{3+} ion has a luminescence band with a maximum at 610 nm and a mono-exponential kinetics with $\tau_r = 3\,\mu s$. Figure 1.3 compares the radioluminescence spectra of BGO and $YAlO_3$:Ti^{3+} (0.2 at. %). The room temperature light yield of Ti^{3+} doped crystal is 30% higher than that of BGO. Al_2O_3:Ti^{3+} crystal codoped with Ca has also an intense luminescence in the near IR with a maximum at 780 nm and a decay time $\tau_r = 4.3\,\mu s$. It has a high scintillation yield [61] and is optimally combined with semiconductor photo-detectors with high sensitivity in the IR region [62].

Ion of vanadium V^+ ($3d^4$) shows an IR luminescence in narrow band gap compounds [63]. The oxide compounds doped with vanadium ions of other valence states V^{2+} ($3d^3$), V^{3+}($3d^2$), V^{4+}($3d^1$) do not show an intense radioluminescence in the visible region at room temperature. Alcali-vanadates,

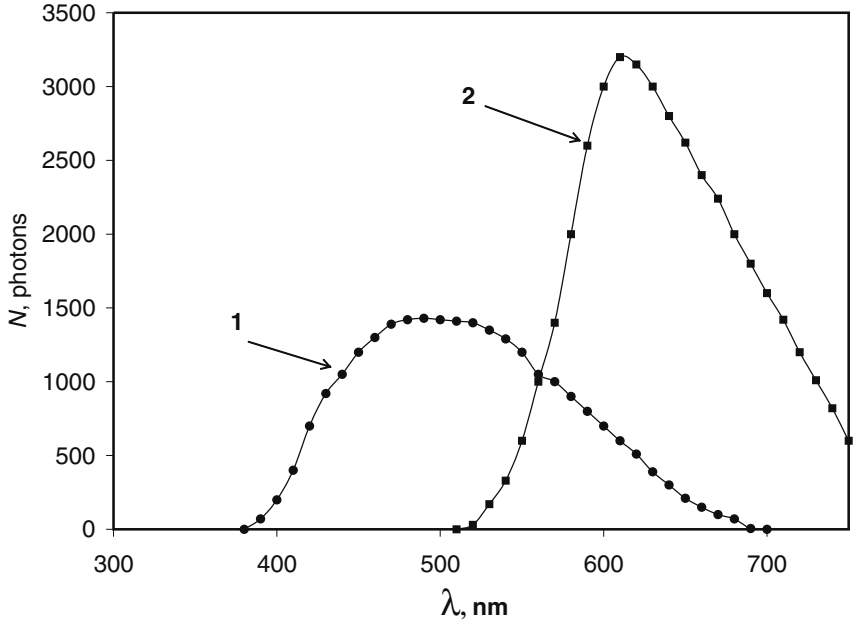

Fig. 1.3. Radioluminescence spectra of BGO (1) and $YAlO_3$:Ti (2) crystals at $T = 300\,K$

where the vanadium ion is in its maximum oxidation state V^{5+}, have an intense cathodoluminescence and are used as luminophore. Double vanadates also exhibit an intense photoluminescence. The luminescence kinetics of double vanadates has a decay time of the order of tens of microseconds at room temperature.

Another well-known activating ion, Cr^{3+} $(3d^3)$, can exhibit a narrow luminescence band at 694 nm due to the $^2E \rightarrow {}^4A_2$ transition, or a wide band in the near-IR region related to the $^4T_2 \rightarrow {}^4A_2$ transition [64], depending on the crystalline field strength in the position of its localization. While crystalline field is weak, the ^{2}E term is lower than the $^4T_2$ term and causes luminescence properties of the material like in ruby. In strong crystalline field in oxygen octahedron, like in emerald, $^4T_2$ level becomes lower showing wide luminescence band. As the $^2E \rightarrow {}^4A_2$ transition is a spin-forbidden transition, the decay kinetics constant is large, of the order of milliseconds. On the other hand, the wide band decays with a characteristic time constant in the microsecond range. $Cr^{4+}(3d^2)$ ion also emits IR luminescence with a decay time constant in the microsecond range in some oxygen compounds [65].

Divalent manganese $Mn^{2+}(3d^5)$ has a strong green luminescence in many compounds with long decay times (milliseconds) because of a spin-forbidden transfer $^4T_1 \rightarrow {}^6A_1$. For instance, Zn_2SiO_4:Mn is one of the best known phosphors [66], which was applied in the first color TVs and is also used in

modern plasma panels. In this compound the Mn^{2+} ion has an intense green luminescence with a maximum near 520 nm and τ_r of about 25 ms.

The trivalent ion of iron $Fe^{3+}(3d^5)$ localized in tetrahedral oxygen coordination is also responsible for a slowly decaying IR luminescence [67]. Its $^4T_1 \rightarrow {}^6A_1$ luminescence can be either directly excited through intracenter transitions or due via a charge transfer process: $O^{2-} \rightarrow Fe^{3+}$ [68]. Iron-doped YAG, $Y_3Al_5O_{12}$:Fe, has radioluminescence spectrum with a peak at 810 nm and a scintillation yield of about 1,000 ph MeV^{-1} at room temperature. The Ni^{2+}-doped crystals also show an intense IR radioluminescence when excited by an electron beam at room temperature [69].

A general drawback of the $3d^n$ ions as activating ions in inorganic scintillator is related to their heterovalence which means that they can change their valence state under ionizing radiation. The localization of their luminescence in the near IR region and the relatively slow decay time of the luminescence are also limiting factors for several applications. It seems that from this group only the Ti^{3+} ion can be considered as a prospective activator if it is in a rather strong crystalline field environment. Apparently, rare-earth aluminium perovskite and some hafnium and zirconium compounds are good host candidates from this point of view.

1.3.2 Ions With s^2 Outer Shell (Mercury-Like Ions)

Ions with s^2 outer shell form a large class of luminescent centers. They are easily introduced into various crystalline compounds which find wide application as phosphors for fluorescent lamps and various fluorescent transducers [70,71]. Ga^+, Ge^{2+}, Se^{4+} with $4s^2$ outer shell; In^+, Sn^{2+}, Sb^{3+}, Te^{4+} with $5s^2$ shell; Hg, Tl^+, Pb^{2+}, Bi^{3+} with $6s^2$ are all in this class. These ions have an intense interconfiguration transition $s^2 \rightarrow sp$ in the vacuum ultraviolet (VUV) range. However the associated luminescence is not observed due to quenching by underlying excited terms $^1P_1$, $^3P_2$, $^3P_1$, $^3P_0$ of s^2-configuration. The intraconfiguration luminescence $^3P_0 \rightarrow {}^1S_0$ is characterized by a large Stokes shift in many compounds and, hence, has strong temperature quenching [72]. The radiant decay time is of the order of hundreds of microseconds at low temperatures but is reduced by three orders of magnitudes (hundreds of nanoseconds) at room temperature by temperature quenching. Moreover the spin–orbit interaction mixes singlet and triplet excited states, reducing further more τ_r in heavy $6s^2$ ions as it is observed for Tl^+, Pb^{2+}, Bi^{3+} ions in an alcali halide and oxide compounds. Ions of s^2 type have played a prominent role in inorganic scintillators development. The discovery of the most widely applied scintillation crystal NaI (Tl) [15] became possible because of the numerous studies of the luminescent properties of the Tl^+ ion in alcali halides. Moreover the first heavy scintillator, BGO, is also the result of systematic investigations of the Bi^{3+} ion in various oxide compounds.

1.3.3 Ion of Molybdenum

Mo doping ion in crystals of tungsten compounds is considered to be a characteristic luminescent center. The Mo impurity substitutes to the tungsten ion in the matrix and forms an anionic complex MoO_4^{2-}, which has a large cross section for electron capture. The properties of the MoO_4^{2-} center and its influence on scintillation parameters of lead tungstate crystal are described in [73, 74].

1.3.4 Uranium Anionic Complexes

Another well-investigated luminescent center is the anionic complex $UO_2{}^{2+}$, which shows a bright green–yellow luminescence in a variety of the crystalline compounds grown from saturated solution [75]. There have been several mentions in the past of a fast luminescence kinetics (nanoseconds) of uranium compounds [76]; however, the majority of the observed uranium doped compounds have a luminescent band with a characteristic decay constant in the microsecond range. Recently it has been shown [77] that the uranyl ion U^{4+} in the $LiYF_4$ crystal has a strong interconfiguration luminescence band $6d5f \rightarrow 5f^2$ in the 240–360-nm region at room temperature. The fast component of the decay $\tau_r = 15$–19 ns dominates in the kinetics. The luminescent properties of the U^{4+} ion have some similarities with those of the Pr^{3+} ion described below.

1.3.5 Rare-Earth Ions

Rare-earth ions are the most frequently used activating luminescent ions. Intraconfiguration luminescent transitions $4f^n \rightarrow 4f^n$ of trivalent ions Pr, Nd, Sm, Eu, Gd, Tb, Dy, Ho, Er, Tm, Yb are widely used in fluorescent lamps, cathode tubes, and lasers [78]. Slow and bright scintillation in the IR region with $\tau_{sc} = 1.9$ ms has been reported in $Y_3Al_5O_{12}$ crystal doped with trivalent ytterbium [79]. The general trend today is to look for fast scintillators. Fast-decaying scintillation in inorganic compounds can be obtained when they are activated by rare-earth ions with the transition $4f^{n-1}5d \rightarrow f^n$. Interconfiguration transitions in trivalent rare-earth ions are allowed both on spin and on parity. They are therefore fast with a decay time constant of $\tau_r = 5$–100 ns. Such trivalent ions are restricted to five rare-earth elements: Ce^{3+} ($4f^1$), Pr^{3+} ($4f^2$), Nd^{3+} ($4f^3$), Er^{3+} ($4f^{11}$), and Tm^{3+} ($4f^{12}$). However the interconfiguration luminescence of Nd^{3+}, Er^{3+}, Tm^{3+} is localized in the region higher than 45,000 cm^{-1} and observed in fluorides only [80]. Moreover, for these three ions there is a strong quenching of this interconfiguration luminescence due to a nonradiating transfer on numerous underlying f levels.

Practically, only two ions, Ce^{3+} and Pr^{3+}, are therefore acceptable activators with a bright and fast scintillation in many compounds. However, the praseodymium ion has, though to a lesser degree, the same problem as

the neodymium ion – a quenching due to nonradiating transitions on lower f levels. Let us consider in more detail the energy-level scheme of trivalent praseodymium ions in a typical fluoride crystal, LaF_3 and in two oxides namely garnet and oxyorthosilicate. They are compared in Fig. 1.4. Contrary to the oxide compounds, the $^1S_0$ level of the f configuration lays below the Stark components of the $5d$ level in fluorides, causing the complete quenching of $4f5d \rightarrow f^2$ Pr^{3+} ion luminescence [81, 82].

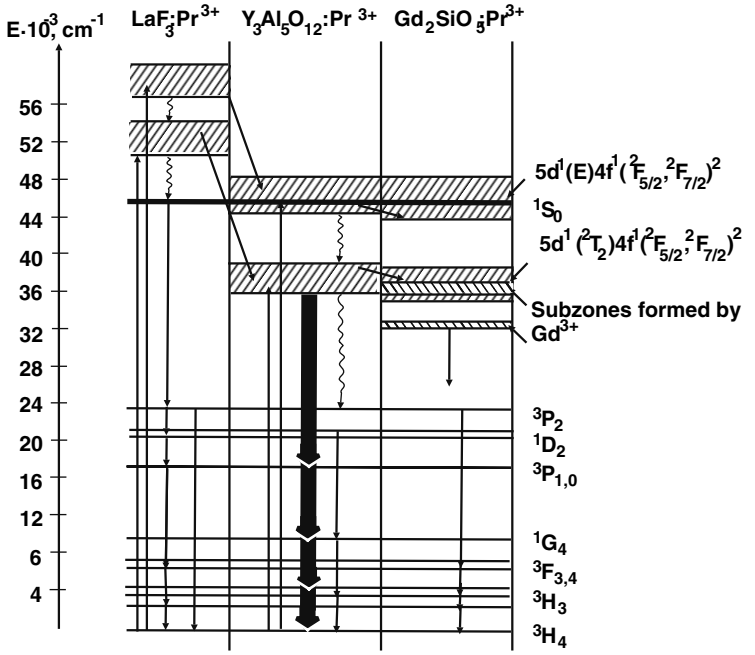

Fig. 1.4. The position of d and f configuration energy levels of Pr^{3+} ion in some crystalline compounds

However, the interconfiguration luminescence is observed as two overlapped wide unstructured bands in many oxide compounds at room temperature for which the host matrix ions do not have energy levels in the forbidden band (for instance, Y, Lu). This is not the case for gadolinium (Gd) where a nonradiative transfer to the subzones formed by the lower excited states $\{^6I_J, ^6P_J, J = 7/2\}$ of Gd^{3+} ions quenches the luminescence.

Ce^{3+} ions have a rather simple structure of energy levels which is shown in Fig. 1.5 according to the data from [83]. The basic $4f$ configuration of the Ce^{3+} ion consists of two spin–orbit components $^2F_{7/2,5/2}$, with an energy difference $\sim$2,400 cm^{-1} As the effect of the crystalline field for the f-orbital of a rare-earth ion is much weaker than the spin–orbit coupling this energy

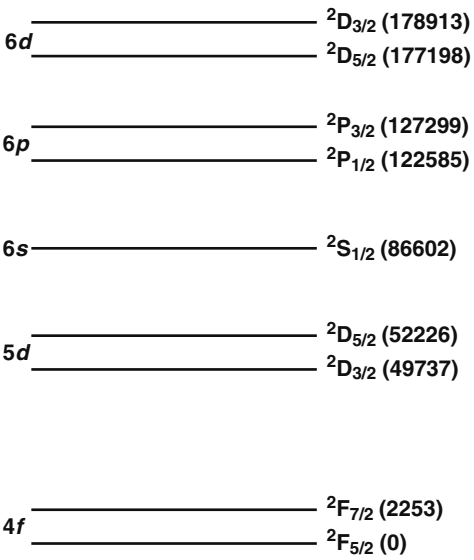

Fig. 1.5. Energy-level structure of free Ce^{3+} ion. Energy levels are given in cm^{-1}

gap between the components $^2F_{7/2,5/2}$ is approximately the same in many compounds. In contrast, the 5*d*-orbital is strongly influenced by the ligands.

The influence of the type of ligand (nepheloxetic effect) appears as a decrease of the difference between the *d* and *f* energy levels from the free ion value following the sequence of ligands: F^-, Cl^-, Br^-, I^-. The average difference in fluorides is $\sim$45,000 cm^{-1}, in chlorides $\sim$37,000 cm^{-1}, in bromides $\sim$35,000 cm^{-1}, and in iodides $\sim$31,000 cm^{-1} [59]. Oxygen compounds have a mean difference of about 40,000 cm^{-1}; however, one can distinguish several groups as a function of the type of matrix creating the oxy-anionic complex [59] as is shown in Table 1.2.

Table 1.2. Mean energy difference between *d* and *f* configurations of Ce^{3+} ion in oxide compounds in different matrices with an oxy-anionic complex

Anionic Group	SO_4^{2-}	CO_3^{2-}	PO_4^{3-}	BO_3^{3-}	SiO_4^{4-}	AlO_6^{9-}, AlO_4^{5-}
Energy difference (cm^{-1})	43,000	42,000	41,500	40,000	39,000	37,000

The mean luminescence maximum of the $4f^05d^1 \rightarrow 4f^1$ transition decreases following the same sequence of ligands: fluorides $\sim$35,000 cm^{-1}, chlorides $\sim$28,000 cm^{-1}, bromides $\sim$26,000 cm^{-1}, oxides $\sim$24,000 cm^{-1}, and sulfides $\sim$18,000 cm^{-1} [84]. The next upper 6*s* configuration is not subject to

a strong influence of the nepheloxetic effect as the $6d$ configuration is mixed with levels of $6s$ and $6p$ configurations.

Only the $5d$ first excited configuration and its Stark components appear in the forbidden zone in the majority of oxides with the oxy-complexes mentioned before. The symmetry of the ligand polyhedron and the coordination of the Ce^{3+} ion determine the level of the Stark decomposition of the $5d$ configuration. Two sets of bands with maxima at 21,830, 29,400 cm^{-1} and at 38,300, 44,400, 48,780 cm^{-1} are observed in absorption and excitation spectra of $Y_3Al_5O_{12}$ where the Ce^{3+} ion is localized in an eightfold oxygen site with a local symmetry D_2. They correspond to the transitions to the doublet E and to the triplet $^3T_1$ of the $5d$ configuration [85–87]. A separation of the doublet components is also found in $LuBO_3$ with vaterite structure where the Ce^{3+} ion is localized in a position with point symmetry D_{2d}, and components of the doublet have maxima near 27,400 and 29,000 cm^{-1} [88]. In a less visible way the doublet was also found in phosphates YPO_4, $LuPO_4$ [89–91] with absorption and excitation bands around 31,000 and 40,000 cm^{-1} have been measured. The localization of the Ce^{3+} ion is C_1 in rare-earth perovskites and an inverse disposition of the triplet and the doublet was observed in absorption and luminescence excitation spectra. For example, the three components of the triplet are seen in $YAlO_3$ at 33,300, 34,500, 36,360 cm^{-1}, and the two components of the doublet have their maximum at 41,900 and 45,500 cm^{-1}, respectively [92, 93].

The Ce^{3+} is localized in the crystalline structure with a ligand coordination number going from 7 up to 12, leading to a large variation of the crystalline field. Therefore, the five components of the Ce^{3+} ion $5d$ configuration decomposition are observed in various compounds in a wide spectral interval between 50,000 and 17,000 cm^{-1}. The maximum of the corresponding luminescence also varies in a wide range from 35,000 up to 15,000 cm^{-1}.

As the averaged energy difference between the ground and first excited states of Ce^{3+} exceeds 10,000 cm^{-1} in the majority of hosts the luminescence quantum yield for an intracenter excitation is close to 1 at room temperature and up to rather high temperature. For example, the temperature luminescence quenching starts at 500 K in $YAlO_3$:Ce^{3+} [94] only.

Besides the trivalent rare-earth ions discussed here, the divalent Eu^{2+} ion is also subject to a bright interconfiguration luminescence; however, it has a relatively slow kinetics with τ_r about 1 µs [95]. The intense 440 nm $4f^6 5d^1 \rightarrow 4f^7$ luminescence band of the Eu^{2+} ion is found in crystals with a structure of the type MAl_2O_4 (M = Co, Sr) [96]. There is a phosphorescence due to the decay of electron centers and the subsequent excitation of Eu^{2+} ion that makes impossible their application as fast scintillators.

The candidates of choice to design fast-doped scintillators within the rare-earth ions family are therefore the trivalent ions of Ce and Pr.

1.4 Classification of Inorganic Scintillation Materials

Since the discovery of sodium iodide by Hofstadter in 1949, alcali-halide crystals have been the most widely used scintillators in numerous applications ranging from detectors for physics research to industrial and medical imaging devices. But the limits of these crystals, especially in experimental high energy and nuclear physics, became apparent with the development of fast response photodetectors, electronics and acquisition systems in the beginning of the eighties. On the other hand, the fast development of crystallographic production technology as well as the large research effort in the field of laser media based on oxide and fluoride crystalline materials boosted the development of high-temperature production technology of crystals. Luminescent crystalline oxide and fluoride of high quality became available in large quantities. This has led to the discovery of a number of new prospective scintillation materials. With the increase of the number of known inorganic scintillators, several approaches to classify them have been developed. Here we will discuss several classifications of the scintillators and give a list of the developed to date scintillation materials and their properties because many of them will be quoted in chapters bellow.

1.4.1 Classification Based on the User's Requirements

Such a classification would help the end user to quickly identify the best scintillating material for a given application. In this case the parameters of choice are the density, the photo-fraction, the light yield, the decay time, and more generally the scintillation performance in the low – ($E < 10\,\mathrm{MeV}$) or in the high – ($E > 10$ MeV) energy domain. Physicochemical and engineering parameters are also important as well as the conditions of the production as they have a direct impact on the price.

1.4.2 Classification Based on Scintillation Mechanisms

Lempicki [23] has suggested to divide scintillators into two categories: extrinsic and stoichiometric. As the cross-luminescence can be observed in crystals, irrespective of the presence of impurities and stoichiometric composition, it is more comprehensive to introduce three classes, namely, *activated scintillators* on the basis of crystalline compounds doped with activating ions; *self-activated scintillators* where radiating centers are ions, anionic complexes, and various excitonic states from the matrix itself; and *cross-luminescent scintillators*.

Some authors have suggested a classification based on the different types of excitons [97]. However, such an approach mixes in one-class materials very different from each other, like NaI (Tl) and $YAlO_3$:Ce, BGO and CsI.

1.4.3 Classification Based on Structural Types of Crystals

Such a classification involves only the crystallographic structure of the scintillator. This approach has allowed to predict and to produce a number of new scintillation crystals, for example, scintillators with garnet, perovskite, oxyorthosilicate, pirosilicate structure doped with cerium and praseodymium ions. Such classification is rather convenient for material scientists but of little interest for end users.

1.4.4 Classification Based on Specific Features of Materials

It has been frequently reported [29] that compounds with wide bandgap can be considered good candidates for scintillation. This is related to the development of Ce^{3+}-doped scintillation materials. On the other hand, the presence of a wide bandgap is not a necessary condition for scintillation occurrence. It increases only the potential spectral domain of the scintillation as it makes the material transparent in a wider spectral rage.

1.4.5 Combined Classification

We would like to propose here a combined classification taking into account the physicochemical properties of a material, for example, a specific anion of the matrix, with the different mechanisms of scintillation. Following this approach, we can distinguish the two important classes of halides (F, Cl, Br, I) and oxydes. Additional classes of compounds are also related to anions sulfur S, phosphorus P, and selenium Se. Each class is divided into groups which involve different mechanisms of scintillation. A further partition inside each group is based on the structural peculiarities of the compounds and of the different types of luminescent centers.

The proposed classification is oriented on one hand to the user and allows without specific knowledge to spot the potential of a class or group on the basis of given operational parameters. On the other hand, it allows the researchers to identify a set of compounds for future development on the basis of the mechanisms of scintillation. This attempt for a classification of scintillation inorganic crystalline compounds known to the present time and some of their physical and scintillation parameters are shown in Table 1.3. To scintillation parameters we insert in the table density ρ, effective charge Z_{eff}, and absorption length X_0 of the crystalline compounds.

Among the crystals listed in the table fluorides have the largest bandgap $E_g > 7$ eV. This is a condition for a possible observation of cross-luminescence. The best known representative of fluoride cross-luminescent scintillators is BaF_2, with a reasonable light yield. Another interesting cross-luminescent material is CsF with a decay time $\tau_{sc} \sim 2{-}4$ ns, and a luminescence peak at 390 nm. Among the self-activated fluorides CeF_3 has been considered as a good candidate for electromagnetic calorimetry at colliders.

Table 1.3. Inorganic scintillation compounds and their essential properties

Scintillator	ρ ($g\,cm^{-3}$)	Z_{eff}/photo absorp. coeff., 511 keV, cm^{-1}/ X_0, cm	Y ph MeV^{-1}	τ_{sc} (ns)	λ_{max} (nm)	Reference
Fluorides						
Cross-luminescent materials						
$LiBaF_3$	5.2	49.3/0.079/2.11	1,400	0.8	190, 230	98
$KMgF_3$	3.2	14.3/0.0007/8.38	1,400	1.3	140–190	98
$KCaF_3$	3	16.7/0.001/7.65	1,400	2	140–190	98
KYF_4	3.6	30.2/0.011/4.55	1,000	1.9	170	98
$BaLu_2F_8$	6.94	63/0.22/1.25	870	1+slow	313	99, 102
BaF_2	4.88	52.7/0.085/2.03	1,430 9,950	0.6 620	220 310	100
CsF	4.64	53.2/0.086/2.69	1,900	2-4	390	103
RbF	3.6	34.6/0.016/3.6	1,700	1.3	203, 234	98
Self-activated materials						
CeF_3	6.16	53.3/0.11/1.77	4,500	30	330	104, 128
Activated						
BaY_2F_8:Ce	4.97	44/0.04/2.5	980	45+slow	329	99, 102
$BaLu_2F_8$:Ce	6.94	63/0.22/1.35	400	35+slow	330	99, 102
CaF_2:Eu	3.18	16.4/0.045/3.72	21,500	940	435	101
LaF_3:Ce	5.9	50.8/0.09/1.69	2,200	26.5	290, 340	130
LuF_3:Ce	8.3	61.1/0.31/1.1	8,000	23+slow	310	130
Chlorides						
Cross-luminescent materials						
$CsCaCl_3$	2.9	43.6/0.03/4.1	1,400	1	250, 305	98
Self-activated materials						
Cs_2LiYCl_6	3.31	44.5/0.04/5.85	6,535 (1 µs) 22,420 (10 µs)	6,600	305	134
$Cs_2NaCeCl_6$	3,25	50.1/0.047/3.22	11,000	1,000	376	99
Activated materials						
Li_3YCl_6:Ce	2.45	27.4/0.027/8.17	3,305 (1 µs) 6,185 (10 µs)	250 2,300	360, 385	134

(*continue*)

Table 1.3. Cont.

Scintillator	ρ ($g\,cm^{-3}$)	Z_{eff}/photo absorp. coeff., 511 keV, cm^{-1}/ X_0, cm	Y ph MeV_1	τ_{sc} (ns)	λ_{max} (nm)	Reference
$LaCl_3$:Ce	3.86		17,000 (0.5 μs) 40,000 (10 μs)	20,330, 2,200	337, 358	130, 133
$CeCl_3$:Ce	3.9	48.4/0.06/2.02	28,000	23	360	122, 133
$LuCl_3$:Ce	4.	61/0.12/1.98	1,300 (0.5 μs) 5700 (10 μs)	50, 250–350, 4,000	374, 400	130 135 133
K_2LaCl_5:Ce	2.89	44.1/0.025/4.5	25,000	1,000	348	99
$RbGd_2Cl_7$:Ce	3.74	53.9/0.069/2.75	43,000	1,000	370	99
Cs_2LiYCl_6:Ce	3.31	44.5/0.04/5.85	9,565 (1 μs) 18,400 (10 μs)	600 6,000	372, 400	134
$Cs_2NaLaCl_6$:Ce	3.2	49.7/0.045/3.3	5,400	1,000	368	99
$Cs_2NaLuCl_6$:Ce	3.71	56.5/0.079/2.61	5,200	1,000	373	99
Cs_3LuCl_6:Ce	3.79	56.7/0.083/2.27	4,400	1,000	375	99
$Cs_3Lu_2Cl_9$:Ce	4.01	58.6/0.097/2.46	650	100,000	409	99
Bromides						
Cross-luminescent materials have not be found						
Self-activated materials have not be found						
Activated materials						
$LaBr_3$:Ce	5.29	46.9/0.065/1.64	61,000	17-35		145
$LuBr_3$:Ce	5.17	63/0.17/1.29	10,000 (0.5 μs) 24,000 (10 MKS)	32,450–550, 5,000	408, 408	130 133
$RbGd_2Br_7$:Ce	4.8	50.6/0.070/2.03	54,700	66	420	99
Cs_2LiYBr_6:Ce	4.15	45.2/0.046/2.15	25,000	72+slow	388	145
K_2LaBr_5:Ce	3.9	42.8/0.035/2.3	40,000	100	359	145
$RbLu_2Br_7$:Ce	4.8	53.6/0.099/1.92	30,000	80+slow	420	130
Iodides						
Cross-luminescent materials have not be found						
Self-activated materials						
CsI	4.51	54/0.09/2.43	16,800	10	310	101
CaI_2	3.96	51.1/0.065/2.29	86,000	550	410	105
HgI_2	6.38	68.8/0.27/1.13	6,000	2,100	580	106
Activated materials						
NaI:Tl	3.67	50.8/0.058/2.56	43,000	230	415	107
CsI:Tl	4.51	54/0.09/2.43	51,800	1,000	560	101
CsI:Na	4.51	54/0.09/2.43	38,500	630	420	101

Table 1.3. Cont.

Scintillator	ρ ($g\,cm^{-3}$)	Z_{eff}/photo absorp. coeff., 511 keV, cm^{-1}/ X_0, cm	Y ph MeV_1	τ_{sc} (ns)	λ_{max} (nm)	Reference
LaI_3:Ce	5.6	54.2/0.12/1.52	200–300	1–2	452, 502	140
LuI_3:Ce	5.6	60.4/0.17/1.35	50,000	31(69%) 400(15%) 3,000(16%) + slow	475, 520	141
K_2LaI_5:Ce	4.4	52.5/0.084/1.91	57,000	24	401	145
CaI_2:Eu		50.6/0.065/2.29	86,000	790	470	105
LiI:Eu	4.08	40.8/0.073/2.73	12,900	1,400	470	101
Sulfides						
Cross-luminescent materials have not be found						
Self-activated materials have not be found						
Activated materials						
CdS:Te	4.8	48/0.051/2.15	17,000	270+slow	640 580	108
Gd_2O_2S:Pr,Ce,F	7.34	61.1/0.214/1.13	40,000	2,100	580	109
Lu_2S_3:Ce	6.2	66.7/0.241/1.25	28,000	32	592	110
$PbSO_4$	6.1-6.4	70.4/0.34/1.3	5,500	1.8, 19 95	340, 380	142 143
Oxides						
Cross-luminescent materials have not be found						
Self-activated materials						
BeO	2.86	8.1/0.0003/7.3	6,500	18	250	123, 125
Y_2O_3	5.04	36/0.019/3.02	15,480	28	370	125
$Y_3Al_5O_{12}$	4.55	30.1/0.014/3.6	11,610	100	260	125
$YAlO_3$	5.35	32/0.02/4.1	9,000	2, 60,2000	308	55, 127
$LuAlO_3$	8.34	64.9/0.29/1.1	13,000	2, 70, 2500	310	
$(Y_{0.3}$-$Lu_{0.7})AlO_3$	7.1	60/0.21/1.3	13,000	2, 70, 3000	310	
Sc_2SiO_5	3.2	16.8/0.0007/10.98	10,600	15	320	124
$NaZrSiO_5$	4.3	30/0.013/3.72	5,600	110, 580	290, 520	124
Lu_3(Al-Sc)$_5O_{12}$	6.7	62.9/0.2/1.41	22,500	610	270	112
$CaMoO_4$: La, Nb		35.2/0.02/1.97	7,500	18,000	530	This book
$CdWO_4$	7.9	64.2/0.262/1.21	19 700	2,000	495	111
$ZnWO_4$	7.87	62.5/0.266/1.19	21,500	22,000	480	121
$CaWO_4$	6.1	63.8/0.221/1.50	6,000	6,00	430	122
$PbWO_4$	8.28	75.6/0.485/0.89	100	6	420	129
$Bi_3Si_4O_{12}$	7.12	74.4/1.15	1,200	100	480	124
$Bi_3Ge_4O_{12}$	7.13	75.2/0.336/1.12	8,200	300	505	111
Activated materials						
LiLuSiO$_4$: Ce	5.61	63.4/0.178/1.68	23,000	41+slow	405	99
$Rb_3Lu(PO_4)_2$:Ce	4.7	49.6/0.077/2.4	30,000	34+slow	420	110
$K_3Lu(PO_4)_2$:Ce	4	51/0.072/3.13	50,000	37+slow	410	110
$Gd_3Sc_2Al_3O_{12}$:Ce	5.56	55.5/0.11/1.93	1,100	108	550	99
$Y_3Al_5O_{12}$:Ce	4.55	32.6/0.017/3.28	11,000	70	550	122

(*continue*)

Table 1.3. Cont.

Scintillator	ρ ($g\,cm^{-3}$)	Z_{eff}/photo absorp. coeff., 511 keV, cm^{-1}/ X_0, cm	Y ph MeV_1	τ_{sc} (ns)	λ_{max} (nm)	Reference
$Y_3Al_5O_{12}$:Pr	4.55	32.6/0.017/3.28	9,250	23.4	310, 380	119
$Lu_3Al_5O_{12}$:Ce	6.7	62.9/0.205/1.41	14,000	100	520	131
Lu_3(Al-Sc)$_3O_{12}$:Pr	6.7		10,000	610	320, 370	112
$YAlO_3$:Ce	5.35	32/0.019/2.2	16,200	30	347	114
$YAlO_3$:Pr	5.35	32//0.019/2.2	7,050	13.3	260, 295	113
($Y_{0.3}$-$Lu_{0.7}$) AlO_3:Ce	7.1	60/0.21/1.3	13,000	18/80/450	375	118
$GdAlO_3$:Ce	7.15	56.2/0.17/1.34	9,000	4/180	335, 358	116, 117
$LuAlO_3$:Ce	8.34	64.9/0.29/1.1	11,400	16/80/520	375	115
Y_2SiO_5:Ce	4.45	35/0.014/3.23	9,200	42	420	126
Y_2SiO_5:Pr	4.45	35/0.014/3.23	4,580	6.5, 33	270, 305	119
$Lu_2Si_2O_7$:Pr	6.23	64.4/0.21/1.39	6,000	15	260, 300	144
Gd_2SiO_5:Ce	6.71	59.4/0.175/1.36	12,500	60, 600	430	107, 120
Lu_2SiO_5:Ce	7.4	66/0.28/1.1	27,000	40	420	126
$Lu_2Si_2O_7$:Ce	6.23	64.4/0.21/1.39	30,000	30	380	132
$La_2Be_2O_5$:Ce		51.5/0.14/1.62	4,300	65	470	124
$LuBO_3$:Ce	7.4	64.5/0.28/1.32	26,000	39	410	110
$Li_6Gd(BO_3)_3$:Ce	3.5	47.9/0.051/4.13	17,000		390	110

Remark. The properties of the scintillating materials listed in the table are at room temperature.

However, its relatively small radiation length X_o ia a major drawback for very large detectors which need to be as compact as possible (see the next chapter). Among the rare-earth ion-doped crystals, CaF_2:Eu and to some extent LuF_3:Ce have a high-light yield, comparable to oxyde crystals. But only LuF_3:Ce has a fast component of the scintillation. Till now, no more effective scintillation cross-luminescent materials have been found among fluorides. A limiting property of fluorides, with the exception of LuF_3 and $BaLu_2F_8$, is their rather low density which restricts their application to low-energy particles and γ-quanta detection.

Chlorides and bromides are characterized by a smaller value of the band-gap E_g and no cross-luminescence at the exception of $CsCaCl_3$ [136]. On the other hand, several high-light yield scintillators have been found in these classes of materials such as $RbGd_2Cl_7$:Ce, $LaCl_3$:Ce, $LuBr_3$:Ce, $RbGd_2Br_7$:Ce [137]. Similar to fluorides, chlorides and bromides have a relatively low density.

Iodides of alkali elements are till now the most frequently used scintillation materials. They are rather light, but are among the brightest known scintillators when doped with Thallium for iodides or in the case of isovalent

substitution of Cs by Na. Their decay time is in the range of hundreds of nanoseconds. Undoped CsI has about the same radiation length as BaF_2 and its scintillation is rather fast. It is therefore a good candidate for high-flux particle physics when a very high density is not mandatory. LiI compound is also a promising scintillation material to detect neutrons.

Sulfides, besides their historical role with ZnS being the first scintillator used for the discovery of α particles, are again at the center of brisk discussions, because of the nice properties of fast and bright red scintillation of Lu_2S_3 doped with Ce^{3+} ions.

Scintillators based on oxide compounds have several advantages. First of all, in an oxygen environment, they are much more stable than halides and particularly fluoride crystals. Thus the majority of oxide single crystals which are potentially applicable as scintillators are rugged, not hygroscopic and chemically inert. Oxygen compounds can have a very high density of 7–10 $\mathrm{g\,cm^{-3}}$ and open new perspectives for detection systems for high-energy γ-quanta.

References

1. Broser VI, Kallmann H (1947) Uber die Anregung von Leuchtstoffen durch schnelle Korpuskularteilchen I. Z Naturforschg 2a:439–440
2. Marshall FH, Coltman JW (1947) The photo-multiplier radiation detector. Phys Rev 72:528
3. Coltman JW, Marshall FH (1947) Some characteristics of the photo-multiplier radiation detector. Phys Rev 72:528
4. Moon RJ (1948) Inorganic crystals for the detection of high energy particles and quanta. Phys Rev 73:1210
5. Kallmann H (1949) Quantitative measurements with scintillation counters. Phys Rev 75:623–626
6. Collins GB, Hoyt RC (1948) Detection of beta-rays by scintillations. Phys Rev 73:1259–1260
7. Bell PR (1948) The use of anthrance as a scintillation counter. Phys Rev 73:1405–1406
8. Kallmann H (1950) Scintillation counting with solutions. Proc Phys Soc (London) Letters to the Editor, pp 621–622
9. Kallmann H, Furst M (1950) Fluorescence of solutions bombarded with high energy radiation (energy transport in liquids). Phys Rev 79:857–870
10. Kallmann H, Furst M (1951) Fluorescence of solutions bombarded with high energy radiation (energy transport in liquids). Part II. Phys Rev 81:853–864
11. Kallmann H, Furst M (1951) High energy induced fluorescence in organic liquid solutions (energy transport in liquids). Part III. Phys Rev 85:816–825
12. Reynolds GT (1950) Noble gas scintillation under electron excitation. Nucleonics 6:488–489
13. Swank RK (1954) Recent advances in theory of scintillation phosphors. Nucleonics 12:14–22
14. Schorr MG, Torney FL (1950) Solid non-crystalline scintillation phosphors. Proc Phys Soc (London) Letters to the Editor, pp 474–475

15. Hofstadter R (1949) The detection of gamma-rays with thallium-activated sodium iodide crystals. Phys Rev 75:796–810
16. Ed A.M. Prokhorov (1998) (In Russian) Physics Encyclopedia Big Russian Encyclopedia, 5:41
17. Fünfer E, Neuert H (1959) Zalhrohre und szcintillationszzäller. Verlag G. Braun, Karlsruhe
18. Cherenkov PA (1934) A visible radiation of pure liquids under γ-radiation. Doclady AN USSR 2:451 (in Russian)
19. Klienknecht K (1987) Detektoren fur Teilchenstrahlung. BG Teubner, Stuttgart
20. Vasiliev A (2000) Relaxation of hot electronic excitations in scintillators:account for scattering, track effects, complicated electronic structure. In: Mikhailin VV (ed) Proc of the Fifth Int Conf on Inorganic Scintillators and Their Applications, SCINT99. Moscow State University, Moscow, pp 43–52
21. Khruchinski A, Korzhik M, Lecoq P (2002) The phenomenon of scintillation in solids. Nucl Instr Meth Phys Res A486:381–384
22. Rodnyi P, Dorenbos P, van Eijk CWE (1995) Energy loss in inorganic scintillators. Phys Stat Sol (b) 187:15–29
23. Lempicki A (1995) The physics of inorganic scintillators. J Appl Spectroscopy 62:209
24. Robbins DJ (1980) On predicting of maximum efficiency of phosphor systems excited by ionizing radiation. J Electrochem Soc 127:2694–2702
25. Van Roosbroeck W (1965) Theory of the yield and Fano factor of electron–hole pairs generated in semiconductors by high-energy particles. Phys Rev A139:1702–1716
26. Lempicki A, Wojtowicz AJ, Berman E (1993) Fundamental limits of scintillator performance. Nucl Instr Meth Phys Res A333:304–1311
27. Rodnyi PA (1997) Physical processes in inorganic scintillators. CRC Press
28. Wojtowicz AJ, Berman E, Lempicki A (1992) Stoichiometric cerium compounds as scintillators, II CeP_5O_{14}. IEEE Trans Nucl Sci NS-39:1542–1548
29. Nikl M (2000) Wide band gap scintillation materials: progress in the technology and material understanding. Phys Stat Sol (a) 178:595–620
30. Becker J, Belski AN, Boutett D et al. (1993) Relaxation of electronic excitations in wide bandgup insulators. In: De Notaristefani F, Lecoq P, Scneegans M (eds) Heavy scintillators for scientific and industrial applications. Frontieres, pp 118–125
31. Vasil'ev AN (1993) Final stages of inelastic electron scattering: influence of scintillation efficiency. In: De Notaristefani F, Lecoq P, Scneegans M (eds) Heavy scintillators for scientific and industrial applications. Frontieres, pp 126–129
32. Ershow N, Zacharov NG, Rodny PA (1982) Spectral-kinetic study of the intrinsic-luminescence characteristics of a fluorite-type crystal. Optica Spectroskopy 53:89–93 (in Russian)
33. Gudovskikh VA, Ershow NN, Krasilnikov SB et al. (1982) Emission of Singlet and Triplet Excitons in Fluorite-Type Crystals under X-ray Excitation. Optics Spectroscopy 53:910–916 (in Russian)
34. Jansons JL, Krumiens V, Rachko ZA et al. (1987) Luminescence due to radiative transitions between valence band and upper core band in ionic crystals (Crosluminescence). Phys Stat Sol (b) 144:835–844

35. Murk V, Namozov B, Yaroshevich N (1995) Complex oxides: electron excitation and their relaxation. Radiat Measure 24:371–374
36. Lushchik A, Murk M, Lushchik Ch et al. (2000) Luminescence of free and self trapped excitons in wide-gap oxides. J Luminescence 87–89:232–234
37. Luschik A, Savkin F, Tokbergenov I (2003) Electron and hole intraband luminescence in complex metal oxides. J Luminescence 102–103:44–47
38. Lecoq P, Dafinei I, Auffray E et al. (1994) Lead tungstate ($PbWO_4$) scintillators for LHC EM-calorimetry. Preprint CERN-PPE/94-225, CMS TN/94-308, December 1994
39. Henderson B, Imbusch GF (1989) Optical spectroscopy of inorganic solids. Clarendon, Oxford
40. Förster TZs (1949) Experimentelle und theoretische untersuchung des zwischenmolekularen ubergangs von elektronenanregungsenergie. Naturforsch 1049 4a:321–332
41. Voronko YuK, Mamedov TG, Osiko VV et al. (1976) Luminescence quenching in garnets doped with trivalent RE JETP 12:478–496 (in Russian)
42. Baryshevsky VG, Drobyshev GYu, Fedorov AA et al. (1992) Rare-earth aluminum perovskite scintillators. In: De Notaristefani F, Lecoq P, Scneegans M (eds) Heavy scintillators for scientific and industrial applications. Frontieres, pp 195–200
43. Dorenbos P, Visser R, van Eijk CWE et al. (1993) Scintillation properties of some Ce^{3+} and Pr^{3+} doped inorganic crystals. In: IEEE NS Symposium, Orlando, USA, 1992 Conference record l:281–285
44. Korzhik M (2000) Scintillators on a base of oxide crystals, inorganic scintillators and their applications In: Mikhailin VV (ed) Proc of the Fifth Int Conf on Inorganic Scintillators and Their Applications, SCINT99. Moscow State University, Moscow, pp 97–105
45. Smirnova SA, Kazakova LI, A Fyodorov AA et al. (1994) Fast and heavy $GdAlO_3$:Ce Scintillators. J Luminescence 60–61:960–962
46. Dijardin C, Pedrini C, Blanc W et al. (1998) Optical and scintillation properties of large LuAlO:Ce^{3+} crystals. J Phys: Condens Matter 10:3061–3073
47. Suzuki H, Tambrello TA, Melcher CL et al. (1992) UV and gamma-ray excited luminescence of Ce doped rear-earth oxyortosilicates. Nucl Instr Meth Phys Res A320:263–272
48. Van Eijk NWE (2001) Inorganic-scintillator development. Nucl Instr Meth Phys Res A460:1–14
49. Bersuker IV, Polinger VZ (1983) Vibronic interaction. Nauka, Moscow (in Russian)
50. Tanabe Y, Sugano SJ (1954) On the absorption spectra of complex ions II. Phys Soc Jap 9:753–766; 9:766–779
51. Vansovski SV (ed) (1969) The theory of crystalline field and optical spectra of impurity ions with notfilled 3d shell. Nauka, Moscow (in Russian)
52. Morrison CA (1980) Host dependence of the rare-earth ion energy separation $4f^N - 4f^{N-1}$ nl. J Chem Phys 72:1001–1002
53. Bettinelli M, Moncorge R (2001) Correlation between the 5d-level position of Ce^{3+} and of the other Ln^{3+} ions in solids. J Luminescence 92:287–289
54. Dorenbos P (2000) The $4f^n \leftrightarrow 4f^{n-1}5d$ transitions of the trivalent lanthanides in halogenises and chalcogenides. J Luminescence 91:91–106
55. Korzhik M, Trower WP (1995) Origin of scintillation in cerium doped oxide crystals. Appl Phys Lett 66:2327–2328

56. Murk V, Kuznetsov A, Namosov B et al. (1994) Relaxation of electronic excitations in YAG and YAP crystals. Nucl Instr Meth Phys Res B91:327–330
57. Bartham RH, Lempicki A (1996) Efficiency of electron–hole pair production in scintillators. J Luminescence 68:225–240
58. Dorenbos P (2001) 5d-level energies of Ce^{3+} and the crystalline environment III. Oxides containing ionic complexes. Phys Rev B 64:125117–1–125117-12
59. Dorenbos P (2002) 5d-level energies of Ce^{3+} and the crystalline environment IV, Aluminates and. simple. Oxides. J Luminescence 99:283–302
60. Balhausen D (1964) Introduction in a ligand fuield theory. Mir, Moscow (in Russian)
61. Krivonosov E, Litvinov LA, Ryzhikov VD (1997) Scintillator based on Al_2O_3. Functional Materials 4:602–604
62. Globus ME, Grinev BV (2000) Inorganic scintillators. New and traditional materials. Akta, Kharkov (in Russian)
63. Goetz G, Pohl UW, Schulz H-J et al. (1994) Spectroscopic detection of the V^+ (d^4) acceptor state im zinc selenide and zinc sulfide. J Luminescence 60–61:16–20
64. McDonagh CJ, Glinn TJ, Imbush GF et al. (1994) Luminescent properties of Cr^{3+} doped $LaSr_2Ga_{11}O_{20}$. J Luminescence 60–61:154–157
65. Baryshevsky VG, Korzhik MV, Kimaev AV (1990) Laser based on a forsterite doped with chromium with tunable wavelenght in niar IR range. J Appl Spectroscopy 53:7–9
66. Bratkar VB, Omanwar SK, Moharil S (2002) Combustion synthesis of the Zn_2SiO_4:Mn Phosphor. Phys Stat Sol (a) 1991:272–276
67. Korzhik MV (1990) Influence of trivalen iron ion on spectroscopic and laser properties YAG:Nd and alumosilicate glasses doped with trivalen rare earth ions. Ph.D. Thesis, Belarussian State University (in Russian)
68. Korzhik MV, Zotov NI, Livshits MG et al. (1988) On the origin of charge transfer transitions $O^{2-} \rightarrow Fe^{3+}$ in doped garnet crystals. J Appl Spectroscopy 48:972–975 (in Russian)
69. Walker G, Kamaluddin B, Glinn TJ et al. (1994) Luminescence of Ni^{2+} centers in forsterite (Mg_2SiO_4). J Luminescence 60–6:123–126
70. Butler KH (1980) Fluorescent lamp phosphors:technology and theory. Pensilvania State University Press, University Park
71. Blasse G, Grabmaier C (1994) Luminescent materials. Springer-Verlag, Berlin
72. Van Den Brand-Folkerts HF (1996) Luminesece of the lead ion in the solids. Thesis, Utrecht
73. Bohm M, Borisevich AE, Drobychev GYu (1997) Influence of Mo impurity on the spectroscopic and scintillation properties of $PbWO_4$ crystals. LAPP Preprint, LAPP-EXP-97 13 December 1997
74. Annenkov A, Bohm M, Borisevich A et al. (2000) Thermally stimulated luminescence properties of lead tungstae crystals, inorganic scintillators and their application In: Mikhailin VV (ed) Proc of the Fifth Int Conf on Inorganic Scintillators and Their Applications, SCINT99. Moscow State University, Moscow, pp 619–626
75. Volodko LV, Komiak AI, Ymreiko DS (1981) Uranium compounds (spectra and strucutre). Belarussian State University, Minsk, pp 1–620
76. Gaviola E, Pringsheim P (1927) Fluorescence of the uranium salts. Z Phys 43:384–386

77. Kirm M, Krupa JS, Makhov VN et al. (2003) 6d5f and 5f^2 configurations of U^{4+} doped into $LiYF_4$ and YF_3 crystals. J Luminescence 104:85–92
78. Shionoya S, Yen WM (1998) Phosphor handbook. Boca Raton, FL, CRS Press, New York
79. Antonini P, Belogubov S, Bressi G et al. (2002) Infrared scintillation of Yb (10%):YAG crystal. Nucl Instr Meth Phys Res A486:799–802
80. Van Pieterson L, Reid MF, Wegh RT et al. (2001) $4f^n \leftrightarrow 4\ f^{n-1}5d$ transitions of the trivalent lanthanides: experiment and theory. J Luminescence 94–95:79–83
81. Loh E (1965) $^1S_0$ level of Pr^{3+} in crystals of fluorides. Phys Rev A 140:1463–1466
82. Caspers HH, Rast HE, Buchanan RA (1965) Energy levels of Pr^{3+} in LaF_3. J Chem Phys 43:2124–2128
83. Eliashevich MA (1953) Rare earth spectra. Nauka, Moscow (in Russian)
84. Dorenbos P (2002) Light output and energy resolution of Ce^{3+} doped scintillators. Nucl Instr Meth Phys Res A486:208–213
85. Autrata R, Schauer P, Kvapil J et al. (1978) A single crystal of YAG—New fast scintillator in SEM. Phys E 11:707–711
86. Presioza (1995) Co YAP:Ce, YAG:Ce scintillators data sheet, Turnov, Czech Republik
87. Tomiki T, Koohatsu T, Shimabukuro H et al. (1992) Ce^{3+} centers in $Y_3Al_5O_{12}$ (YAG) single crystals II. Phys Soc Japan 61:2382–2387
88. Zhang L (1998) Elaboration et propriétés de luminescence et de scintillation de matériaux denses à base de lutécium dopés aux ions cérium et praséodyme. Ph.D. Thesis, l: Universite Claude Bernard-Luon I, France
89. Karanjikar NP, Naik RC (1988) X-ray excited optical luminescence of Ce^{3+} in YPO_4 and location of 5d levels. Solid State Comm 65:1419–1422
90. Ropp RC (1968) Phosphors based on rare earth phosphates. I. Spectral properties of some rare earth phosphates. J Electrochem Soc 115:841–845
91. Williams GM, Edelstein N, Boatner LA et al. (1989) Anomalously small 4f–5d oscillator strengths and 4f–4f electronic Raman scattering cross sections for Ce^{3+} in crystals of $LuPO_4$. Phys Rev B 40:4143–4152
92. Baryshevski VG, Davidchenko AG, Korzhik MV et al. (1990) Fast scitillation crystals for detectors of ionizing radiation. JETP Letters 16:75–78
93. Weber MJ (1973) Optical spectra of Ce^{3+} fluorescence in $YAlO_3$. J Appl Phys 44:3205–3208
94. Lyu LJ, Hamilton DS (1991) Radiative and non-radiative relaxation measurements in Ce^{3+} doped crystals. J Luminescence 48–49:251–254
95. Hoshina T (1980) 5d $\geq$ 4f radiative transition probabilities of Ce^{3+} and Eu^{2+} in crystals. J Phys Soc Jpn 48:1261–1268
96. Aitasalo T, Holsa J, Jungner H et al. (2001) Mechanism of persistent luminescence in Eu^{2+}/RE^{3+} doped alkaline earth aluminates. J Luminescernce 94–95:59–63
97. Belski AN (2000) Localization and interaction of electronic excitations are created by Renthen synchrotron radiation in inorganic scintillators. Ph.D. Thesis, Moscow State University (in Russian)
98. Van Eijk CWE, Andriessen J et al. (1993) Experimental and theoretical studies of cross luminescence In: De Notaristefani F, Lecoq P, Scneegans M (eds) Heavy scintillators for scientific and industrial applications. Frontieres, pp 161–166

99. Van't Spijker JC (1999) Luminescence and scintillation of Ce^{3+} doped inorganic materials for gamma-ray detection. Thesis, Delft University Press
100. Optical crystals Merck Ltd catalog (1992)
101. Scintillation detectors Crismatec Saint Gobain Catalog (1992)
102. Van't Spijker JC, Dorenbos P, van Eijk CWE et al. (1999) Luminescence and scintillation properties of BaY_2F_8:Ce^{3+}, $BaLu_2F_8$ and $BaLu_2F_8$:Ce^{3+}. J Luminescence 85:11–19
103. Moszunski M, Allemand R, Laval M et al. (1983). Recent progress in fast timing with CsF scintillators in application to time—Of-flight positron tomography in medicine. Nucl Instr Meth Phys Res 205:239–249
104. Wojtowich AJ, Balcerzuk M, Berman E et al. (1994) Optical spectroscopy and scintillation mechanisms of $Ce_xLa_{1-x}F_3$. Phys Rev B49:14880–14895
105. Hofstadter R, O'Dell EW, Schmidt CT (1964) CaI_2 and CaI_2 (Eu) scintillation crystals. Rev Sci Instrum 35:246–247
106. Shulgin B, Gorkunova SI, Petrov VL et al. (1996) Some scintillation properties of HgI_2 single crystals. In: Dorenbos P, van Eijk CWE (eds). Inorganic scintillators and their application. Delft University Press, pp 459–461
107. Sakai E (1987) Recent measurements on scintillator–photodetector systems. IEEE Trans Nucl Sci NS-34:418–422
108. Scotanus P, Dorenbos P, Ryzikov VD (1992) Detection of CdS (Te) and ZnS (Tl) scintillation light with silicon photodieds. IEEE Trans Nucl Sci 39:546–550
109. Grabmaier BC, Rossner W, Berthold T (1996) Phosphors in X-ray computed tomography and for the γ-ray Anger camera In: Dorenbos P, van Eijk CWE (eds). Inorganic scintillators and their application. Delft University Press, pp 29–35
110. Van Eijk CWE (1997) New scintillators, new light sensors, new applications. In: Yin Zhiwen, Feng Xiqi, Li Peijun, Xue Zhilin (eds). Proc Int Conf on Inorganic Scintillators and Their Applications, SCINT'97. CAS, Shanghai Branch Press, Shanghai, pp 5–12
111. Holl I, Lorenz E, Mageras G (1988) A measurement of light yield of common inorganic scintillators. IEEE Trans Nucl Sci 35:105–109
112. Dorenbos P, de Haas JTM, van Eijk CWE et al. (1996) Scintillation properties of Pr^{3+} doped $Lu_3Al_{5-x}Sc_xO_{12}$ crystals, inorganic scintillators and their application. In: Dorenbos P, van Eijk CWE (eds). Inorganic scintillators and their application. Delft University Press, pp 365–367
113. Baryshevski VG, Zuevski RF, Korzhik MV et al. (1991) Fast scintillator $YAlO_3$:Pr. JETP Letters 17:82–85 (in Russian)
114. Baryshevsky VG, Korzhik MV, Moroz VI et al. (1991) $YAlO_3$:Ce-fast-acting scintillators for detection of ionizing radiation. Nucl Instr Meth Phys Res B58:291–293
115. Moszunski A, Wolski D, Ludziejewski T et al. (1997) Properties of the new LUAP:Ce scintillator. Nucl Instr Meth Phys Res A385:123–131
116. Dorenbos P, Visser R, van Eijk CWE et al. (1993) Fast scintillating crystals for the detectors of ionizing radiation. IEEE Trans Nucl Sci 40:388–394
117. Dorenbos P, Bougrine E, de Haas JTM et al. (1995) Scintillation properties of $GdAlO_3$:Ce crystals. Radiation Effects Defects Solids 135:321–324
118. Trower WP, Korzhik MV, Fedorov AA et al. (1995) Cerium-doped lutetium-based single crystal scintillators. Inorganic scintillators and their applications.

In: Dorenbos P, van Eijk CWE (eds). Inorganic scintillators and their application. Delft University Press, pp 355–358
119. Dorenbos P, Marsman M, van Eijk CWE et al. (1995) Scintillation properties of Y_2SiO_5:Pr crystals. Radiation Effects Defects Solids 135:325–327
120. Baryshevski VG, Livshits MG, Korzhik MV et al. (1991) Scintillation properties of $Gd_2SiO_5:Ce^{3+}$ crystals. Proseddings AN BSSR 4:114–117 (in Russian)
121. Stavisski YuJa, Shopar AV (1962) Scintillation caunter with crystal CaF_2. IET 5–6:177–178 (in Russian)
122. Derenzo SE, Moses WW (1993) Experimental efforts and results in finding new heavy scintillators. In: De Notaristefani F, Lecoq P, Scneegans M (eds). Heavy scintillators for scientific and industrial applications. Frontieres, pp 125–136
123. Shulgin BV, Kruzalov AV, Ogorodnikov IN (1988) Scintillation properties of BeO single crystals. J Appl Spectroscopy 49:286–291 (in Russian)
124. Shulgin B (1991) Fast inorganic scintillators. In: Proc Int Symp Luminescent detectors and transformers of ionizing radiation (Lumdetr'91). Riga, Latvia A3
125. Ogorodnikov IN, Kruzhalov A, Ivanov VYu (1995) Mechanizms of fast UV scintillations in oxyde crystals with self trapped excitons. In: Dorenbos P, van Eijk CWE (eds). Inorganic scintillators and their application. Delft University Press, pp 216–219
126. Melcher CL, Schweitzer JS, Peterson CA et al. (1995) Crystal growth and scintillation properties of the rare earth oxyorthosilicates. In: Dorenbos P, van Eijk CWE (eds). Inorganic scintillators and their application. Delft University Press, pp 309–316
127. Dorenbos P Private (1995) communication
128. Auffray E (1998) Etudes des mecanismes de scintillation et des modificatios sous irradiation des proprietés du fluorure de cerium en vus de son utilisation en calorimetrie electromagnetique de haute resolution. Thèse de doctorat de l'université Paris VI, specialité:Physique des solides. Paris
129. Annenkov AA, Korzhik M, Lecoq P (2002) Lead tungstate scintillation material. Nucl Instr Meth Phys Res A490:30–50
130. Guillot-Noel O, von Loef ED, Dorenbos P et al. (2000) Luminescence and scintillation properties of Ce^{3+} activited trihalides compounds. In: Mikhailin VV (ed) Proc of the Fifth Int Conf on Inorganic Scintillators and Their Applications, SCINT99. Moscow State University, Moscow, pp 282–287
131. Dorenbos P, Bougrine E (2002) (Private communication) Unpublished data
132. Van Eijk CWE. (1999) Some recent developemts in inorganic–scintillator research. In: Ronda CR, Shea LE, Srivastava AM (eds) Proc Eight Int Symp of Electrochemical Soc. 1999
133. Guillot-Noel O, de Haas JTM, Dorenbos P et al. (1999) Optical and scintillation properties of cerium-doped $LaCl_3$, $LuBr_3$, $LuCl_3$. J Luminescence 85:21–35
134. Van't Spijker JC, Dorenbos P, van Eijk CWE et al. (1999) Optical and scintillation properties pure and of Ce^{3+} doped $CsLiYCl_6$ and $Li_3YCl_6:Ce^{3+}$ crystals. J Luminescence 85:299–305
135. Van't Spijker JC, Dorenbos P, van Eijk CWE et al. (1999) Scintillation and luminescence properties of Ce^{3+} doped K_2LaCl_5. J Luminescence 85:1–10
136. Vasil'chenko VG, Zhmurova ZI, Krivandina EA et al. (2000) New optical multicomponent single-crystal materials based on heavy metal fluorides. IET 43:46–52 (in Russian)

137. Van Spijker JC, Frijns OW, Dorenbos P et al. (1997) $RbGd_2Cl_7:Ce^{3+}$ and $RbGd_2Br_7:Ce^{3+}$ new scintillators with a high light yield. In: Yin Zhiwen, Feng Xiqi, Li Peijun, Xue Zhilin (eds) Proc Int Conf on Inorganic Scintillators and Their Applications, SCINT'97. CAS, Shanghai Branch Press, Shanghai, pp 330–333
138. Shah KS, Glodo J, Klugerman M et al. (2003) LuI_3:Ce—A new scintillator for gamma ray spectroscopy. IEEE Conference Record, N27–7
139. Derenzo SE, Weber MJ, Klintenberg MK (2002) Temperature dependence of the fast, near-band-edge scintillation from CuI, HgI_2, PbI, ZnO:Ga, and CdS:In. Nucl Instr Meth Phys Res A486:214–219
140. Bessiere A, Doenbos P, van Eijk CWE, Kramer KW, Gudel HU, de mello Donega C, Meijrink A (2005) Luminescence and scintillation properties of the small band gup compound $LaI_3:Ce^{3+}$ To be published in Nucl. Instr. Meth. Phys. Res. A (NIMA 26260)
141. Glodo J, Shah KS, Klugerman M, Wong P, Higgins B, Dorenbos P (2005) Scintillation properties of LuI_3:Ce To be published in Nucl. Instr. Meth. Phys. Res. A (NIMA 26316)
142. Moses WW, Derenzo SE, Shichta PJ (1992) Scintillation properties of lead sulfate, IEEE trans. Nucl Sci, 39,5:1190–1194
143. Zadneprovsi BI, Kamenskikh IA, Kolobanov VN, Mikhailin VV, Spinkov IN, Kirm M (2004) Gel growth, luminescence and scintillation of PbSO4 crystals. Inorganic Materials 40,7:735–739
144. Pidol L, Viana B, Kahn-Harari A, Bessiere A, Dorenbos P (in press) Luminescence properties and scintillation mechaisms of Ce^{3+}, Pr^{3+}, and Nd^{3+} doped lutetium pyrosilicate. Nucl Instr Meth Phys Res A (NIMA 26281)
145. Van Loef (2003) Halide scintillators. Thesis, Delft University Press, p 125
146. Dorenbos P, Contribution to the SCINT05 conference on scintillators and their industrial applications, Alushta, Ukraine, Sept. 2005